Scientific paper

Magnetic Nanoparticles Linked to Pyridinium Hydrotribromide Groups as Catalysts for Selective Oxidation of Alcohols and Protection of Alcohols

Sonia Tabari, Ali Reza Pourali* and Ehsan Nazarzadeh Zare

School of Chemistry, Damghan University, Damghan 36715-364, Iran

** Corresponding author: E-mail: pourali@du.ac.ir*
+982335220095; Fax: +982335220095. ORCID: 0000-0002-8918-1818

Received: 02-18-2021

Abstract

In this research, a novel magnetic nanocatalyst based on iron oxide nanoparticles linked with pyridinium hydrotribromide (Fe_3O_4@$PyHBr_3$) was synthesized in three steps. In the first step, 3-(aminopropyl)triethoxysilane (APTES) was reacted with 4-(bromomethyl)pyridine hydrobromide. In the second step, the product obtained in the first step was reacted with iron oxide nanoparticles. In the last step, a grinding reaction was carried out with KBr and HIO4 in a mortar. The Fe_3O_4@$PyHBr_3$ nanocatalyst was characterized by FT-IR, CHN, XRD, SEM, TGA and VSM analysis. The magnetic nanocatalyst was used as a catalyst for the selective oxidation of alcohols to aldehydes and ketones using 30% H_2O_2 as oxidant in a short time and with high yields. Moreover, no overoxidation of the alcohols was observed. The nanocatalyst was efficiently recycled in five consecutive cycles without significant loss of its catalytic activity. Moreover, trimethylsilylation and tetrahydropyranylation of alcohols were carried out in the presence of this nanocatalyst.

Keywords: Magnetic nanoparticles; pyridinium hydrotribromide; oxidation of alcohols; tetrahydropyranylation; trimethylsilylation

1. Introduction

Organic tribromides are widely used as selective bromination reagents for various organic functionalities.[1–6] In addition, they are also used as efficient catalysts for the oxidation of some organic substrates such as alcohols,[7] aldehydes,[8] and sulfides,[9,10] trimethylsilylation[11,12] or tetrahydropyranylation[13] of alcohols, α-thiocyanation[14] or thioacetalization[15] of ketones, and the synthesis of heterocyclic rings.[16] Typical organic tribromides include tetrabutylammonium tribromide (TBATB),[2,9] pyridinium hydrotribromide (PyHTB),[4–6,14] benzyltrimethylammonium tribromide (BTMATB),[7] 2-carboxyethyltriphenylphosphonium tribromide (CTPTB)[11] and benzyltriphenylphosphonium tribromide.[13,15] These reagents have attracted considerable attention in organic synthesis and have proven to be leaders over liquid bromine such as N-bromosuccinimide (NBS), Br_2/HBr and other conventional bromination reagents due to their ease of use, mildness, efficiency and selectivity. They are stable and crystalline solids that can release a stoichiometric amount of bromine. Other advantages include their recoverability and reusability when used as catalysts.

In recent years, much attention has been paid to Br_3^- immobilized on polymers,[1,17] magnetic nanoparticles (MNP)[16,18–23] and other solid supports.[24] The organic tribromide immobilized on magnetic nanoparticles can be easily separated from the reaction mixture using an external magnet without the need for filtration or other workup processes. The use of magnetic nanoparticles (MNP) as a catalyst support enables efficient recovery of the catalyst. This can solve the problems associated with nanoparticle separation.[25,26] Although several immobilized tribromides have been synthesized, in most cases their preparation involves the use of liquid Br_2 and/or HBr,[16,21–24] which leads to an environmental problem.

Numerous improved methods for the synthesis of organic tribromides have been described in the literature and are considered to be environmentally friendly. These improved methods use an oxidation system for the oxidation of organic bromide to organic tribromides, such as $(NH_4)_2S_2O_8/H^+$,[7] $NaOCl/H^+$,[10] $KMnO_4$ /H^+,[11] H_5IO_6,[12] oxone®,[15] MCPBA,[3] H_2MoO_4 or V_2O_5/ H_2O_2,[27,] and CAN.[28] Despite the introduction of these oxidation methods in the literature, many of the recently reported methods for the synthesis of magnetic nanoparticles (MNP)[16,21–23] or polymer-assisted[1,17] bromine sources involve liquid Br_2 and/or HBr, which continues to cause environmental problems. Therefore, the development of newer strategies that do not require the use of molecular bromine or metals and strong mineral acids remains a challenge for the synthesis of immobilized organic tribromides, especially nanoparticle-based magnetic catalysts.

In this work, we reported a novel method for the synthesis of pyridinium hydrotribromide on magnetic Fe_3O_4 nanoparticles (MNPs) by oxidation of immobilized organic bromide to tribromide using periodic acid (H_5IO_6) as a cheap, nontoxic, efficient, and easy-to-use oxidant. Fe_3O_4@$PyHBr_3$ was used as a catalyst for the selective oxidation of alcohols to aldehydes and ketones using 30% H_2O_2. In addition, trimethylsilylation and tetrahydropyranylation of alcohols were carried out in the presence of this catalyst..

2. Experimental Section

2. 1. Instrumentation, Analysis and Raw Materials

All products were known and characterized by comparing their physical data with those of known samples or by their spectral data. Infrared spectra (IR) were recorded on the KBr matrix using a Perkin Elmer RXI spectrometer. Nuclear magnetic resonance (NMR) spectra were recorded in DMSO-d_6 or $CDCl_3$ using tetramethylsilane (TMS) as an internal standard with a Bruker Avance DRX spectrometer. Thermogravimetric analysis (TGA) was performed using a BAHR Thermo analyze STA 503 instrument. XRD patterns were recorded using a Bruker D8-Advance diffractometer. Elemental analysis was performed using a Costech Elemental Combustion System CHNS-O (ECS 4010). Field emission scanning electron microscopy (FESEM) was performed using a MIRA3 TESCAN instrument. A Lakeshore7400 vibratory magnetometer (VSM) was used to characterize magnetic properties at room temperature.

2. 2. Preparation of the Fe_3O_4 Magnetic Nanoparticles (Fe_3O_4 MNP)

Fe_3O_4-MNP were prepared according to the method described in the literature.[29] Typically, $FeCl_3 \cdot 6H_2O$ (5.406 g, 20 mmol) and $FeCl_2 \cdot 4H_2O$ (1.988 g, 10 mmol) were dissolved in distilled water (75 mL) in a three-neck flask (250 mL) under an inert atmosphere. Then NaOH solution (10 M, 10 mL) was added with vigorous mechanical stirring until the pH of the solution was increased to 11. The temperature of the mixture was raised to 80 °C. The mixture was kept in an ultrasonic bath for 1 hour. The black precipitate was separated with a magnet, washed with double-distilled water to neutrality, then washed with ethanol (2 × 20 mL) and dried at 60 °C in a vacuum oven.

2. 3. Synthesis of Fe_3O_4@$PyHBr_3$ MNP

(3-Aminopropyl)triethoxysilane (APTES) (1.771 g, 8 mmol) was dissolved in $CHCl_3$ (10 mL) and then 4-(bromomethyl) pyridine hydrobromide (2.024 g, 8 mmol) was added to the solution. The mixture was heated under reflux for 24 hours. Then the solvent was evaporated and the product (APTES-MPyHBr) was dried. Then magnetic Fe_3O_4 nanoparticles (1.2 g) were added to APTES-MPyHBr (2 g) in toluene (10 mL) and the mixture was heated for 12 hours under N_2 atmosphere under reflux conditions. The magnetic Fe_3O_4@PyHBr nanoparticles were isolated with a magnet, washed with CH_2Cl_2 (3 × 20 mL), and dried at 60 °C in a vacuum oven.

Analytical data for Fe_3O_4@PyHBr: C, 18.65; H, 3.02; N, 4.86%.

A mixture of Fe_3O_4@PyHBr (3 g), KBr (1.27 g, 10.67 mmol), and HIO_4 (2.70 g, 14.07 mmol) were ground in a mortar for 30 min at room temperature. The color of the mixture was changed from orange to dark brown. The Fe_3O_4@$PyHBr_3$ MNPs were washed with H_2O (3 × 15 mL) and then with ethanol (3 × 15 mL) and dried at 60 °C in a vacuum oven. Analytical data for Fe_3O_4@$PyHBr_3$: C, 12.96; H, 1.67; N, 3.65%.

2. 4. Typical Procedures

2. 4. 1. Oxidation of 4-nitrobenzyl Alcohol

Magnetic nanocatalyst Fe_3O_4@$PyHBr_3$ (0.070 g, 0.091 mmol) was added to a mixture of 4-nitrobenzyl alcohol (0.153 g, 1 mmol) and H_2O (1 mL), followed by the addition of hydrogen peroxide (30%, 0.45 mL, 4 mmol), and the resulting mixture was heated to 50 °C. The progress of the reaction was monitored by TLC using n-hexane-ethyl acetate (7:3) as eluent. After completion of the reaction (75 min), the catalyst was separated using a magnet. Then the reaction mixture was extracted with diethyl ether (3 × 5 mL). The organic layer was dried over anhydrous magnesium sulfate and evaporated under reduced pressure to give 4-nitrobenzaldehyde (0.128 g, 0.85 mmol); mp: 104–106 °C.

FT-IR (KBr, cm^{-1}): ν 3107 (w), 3066 (w), 2956(s), 2926 (s), 2854 (s), 1706 (s), 1608 (s), 1544 (s), 1454 (s), 1378 (s), 1360 (s), 1346 (s), 1197 (s), 852 (s), 818 (s), 740 (s).

^{1}HNMR (DMSO-d_6, ppm): δ 8.12–8.17 (m, 2H), 8.39–8.42 (m, 2H), 10.15 (s, 1H).

2. 4. 2. Trimethylsilylation of Benzyl Alcohol

The magnetic Fe_3O_4@$PyHBr_3$ nanocatalyst (0.070 g, 0.091 mmol) was added to a mixture of benzyl alcohol

(0.108 g, 1 mmol) and HMDS (0.113 g, 0.7 mmol) in CH_2Cl_2 (5 mL), and the resulting mixture was mechanically stirred at room temperature. The progress of the reaction was monitored by TLC using n-hexane-ethyl acetate (7:3) as eluent. After completion of the reaction (10 min), the catalyst was separated using a magnet. Then the reaction mixture was extracted with diethyl ether (3 × 5 mL). The organic layer was dried over anhydrous magnesium sulfate and evaporated under reduced pressure to give benzyl trimethylsilyl ether (0.166 g, 0.92 mmol).

Colorless liquid; b.p. 93 °C.

FT-IR (KBr, cm^{-1}): ν 2957, 1250, 1094, 727.

^{1}HNMR ($CDCl_3$, ppm): δ 0.18 (s, 9H), 4.29 (s, 2H), 7.26–7.40 (m, 5H); ^{13}C NMR ($CDCl_3$) δ: 0.09, 70.7, 127.1, 127.3, 129.0, 145.7.

2. 4. 3. Tetrahydropyranylation of 4-chlorobenzyl Alcohol

The magnetic nanocatalyst Fe_3O_4@$PyHBr_3$ (0.070 g, 0.091 mmol) was added to a mixture of 4-chlorobenzyl alcohol (0.143 g, 1 mmol) and DHP (0.126 g, 1.5 mmol) in CH_3CN (5 mL), and the resulting mixture was mechanically stirred at room temperature. The progress of the reaction was monitored by TLC using n-hexane-ethyl acetate (7:3) as eluent. After completion of the reaction (3 h), the catalyst was separated using a magnet. Then the reaction mixture was extracted with diethyl ether (3 × 5 mL). The organic layer was dried over anhydrous magnesium sulfate and evaporated under reduced pressure to afford 4-chlorobenzyl tetrahydropyranyl ether (0.213 g, 0.94 mmol).

FT-IR (KBr, cm^{-1}): ν 3070 (w), 2944(s), 2871 (s), 1442 (m), 1343 (m), 1128 (s), 1029 (s), 754 (s).

^{1}HNMR ($CDCl_3$, ppm): δ 1.57–1.60 (m, 2H), 1.64–1.65 (m, 2H), 1.66–1.78 (m, 2H), 3.56–3.60 (m, 1H), 3.91–3.96 (m, 1H), 4.50–4.52 (d, 1H), 4.72–4.74 (t, 1H), 4.77–4.80 (d, 1H), 7.30–7.36 (m, 4H).

3. Results and Discussion

The synthesis of Fe_3O_4 MNP linked to pyridinium hydrotribromide (Fe_3O_4@ $PyHBr_3$) was carried out in three steps. In the first step, APTES-MPyHBr was synthesized by the reaction of 3-(aminopropyl)triethoxysilane (APTES) with 4-(bromomethyl)pyridine hydrobromide (MPyHBr) in $CHCl_3$ under reflux conditions. In the second step, APTES-MPyHBr was reacted with Fe_3O_4 magnetic nanoparticles to obtain the Fe_3O_4@PyHBr magnetic nanoparticles. In the last step, the mixture of Fe_3O_4@PyHBr, KBr and HIO_4 was ground in a mortar to obtain the magnetic Fe_3O_4@$PyHBr_3$ nanoparticles (Scheme 1).

Fe_3O_4@$PyHBr_3$ was characterized by FT-IR, CHN, XRD, SEM, TGA and VSM analysis. The FT-IR spectra confirmed the preparation of the magnetic nanocatalyst at each step (Figure 1). The FTIR spectrum of Fe_3O_4@ $PyHBr_3$ nanoparticles (Figure 2) showed two sharp absorption

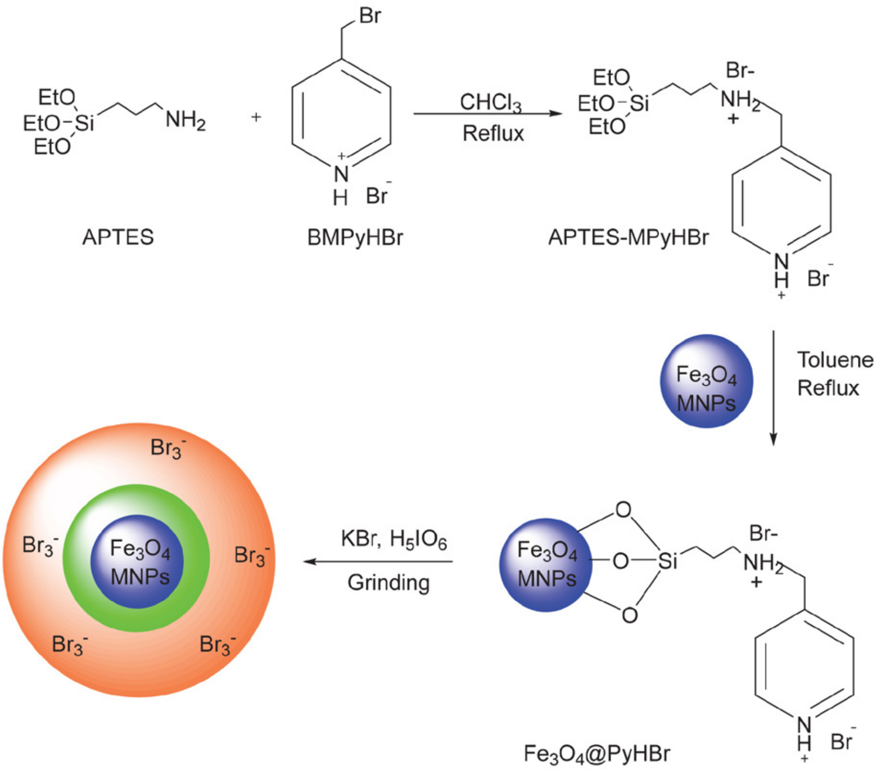

Scheme 1. Synthesis of magnetic Fe_3O_4@$PyHBr_3$ nanoparticles.

bands at 2927 cm^{-1} and 1222 cm^{-1}, which are related to stretching and bending vibrations of CH_2 groups, respectively. The broad absorption bands at 1045 cm^{-1} and 1115 cm^{-1} are related to the stretching vibrations of the Si-O bonds. The absorption band at 3421 cm^{-1} is due to the N-H group overlaid by the hydroxyl group (Fe^3O^4 has a OH -rich surface). In addition, the absorption band at 585 cm^{-1} is due to the stretching vibration of the Fe-O bond in Fe_3O_4.

The elemental analysis results (CHN) showed that the carbon, hydrogen and nitrogen contents of Fe3O4@PyHBr3 were 12.96, 1.67 and 3.65 (wt%), respectively, corresponding to a loading of 1.3 mmol of nitrogen groups (Br3– content) per gram of catalyst. The analytical results of CHN showed that the carbon, hydrogen and nitrogen contents of Fe3O4@PyHBr (monobromide) were 18.65, 3.02 and 4.86 (wt%), respectively. Comparing the total weight percentages of carbon, hydrogen and nitrogen in Fe3O4@PyHBr and Fe3O4@PyHBr3, the ratio is 1.45, which is very close to 1.36, calculated from the chemical formula of the organic segment of these compounds.

X-ray powder diffraction (XRD) analysis was performed to characterize the crystalline structure of Fe3O4@PyHBr3. The XRD pattern of Fe3O4@PyHBr3 showed a semi-crystalline nature compared to the XRD pattern of Fe3O4 (not shown here).[26]

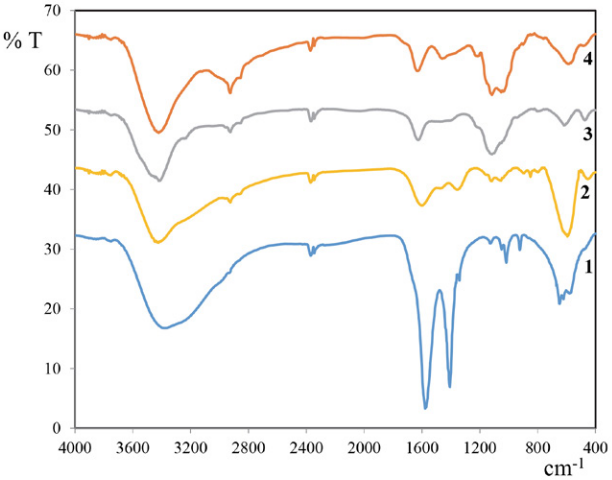

Figure 1. FT-IR spectrum of Fe_3O_4 MNPs (1); Fe_3O_4@ PyHBr MNPs (2); Fe_3O_4@ $PyHBr_3$ MNPs (3); APTES-MPYHBr (4).

The image of the magnetic Fe_3O_4@$PyHBr_3$ nanoparticles in the field emission scanning electron microscope (FESEM) shows a spherical structure with a particle size in the range of 35–40 nm (Figure 4).

The magnetic properties of Fe_3O_4 and Fe_3O_4@$PyHBr_3$ were studied using a vibrating sample magnetometer (VSM) at room temperature. The saturation magnetization of Fe_3O_4@$PyHBr_3$-MNP was about 50 emu g^{-1}, which was

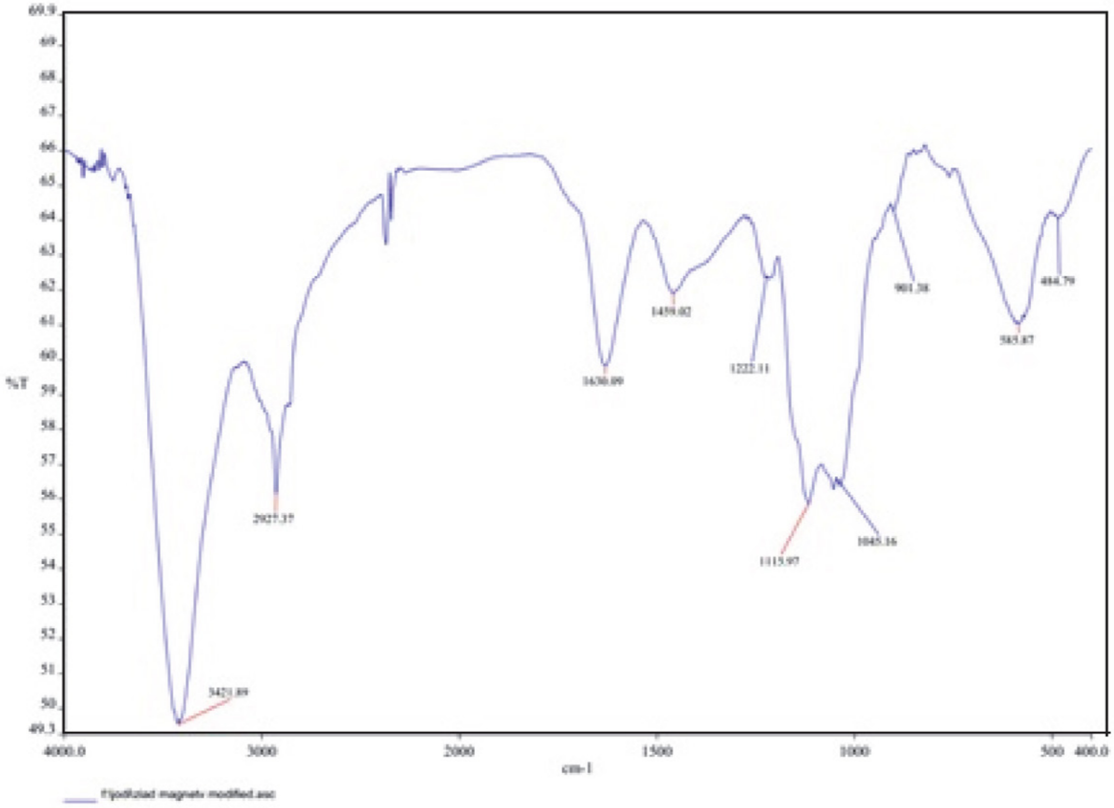

Figure 2. FT-IR spectrum of Fe_3O_4@$PyHBr_3$ MNP (KBr).

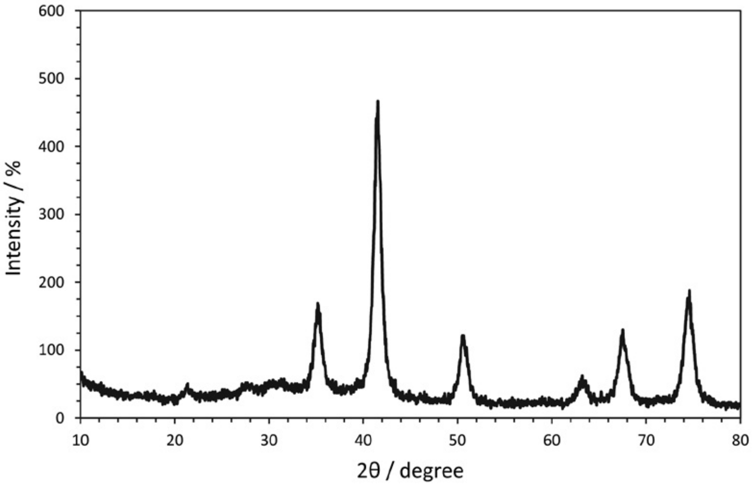

Figure 3. XRD pattern of Fe_3O_4@ $PyHBr_3$ MNP.

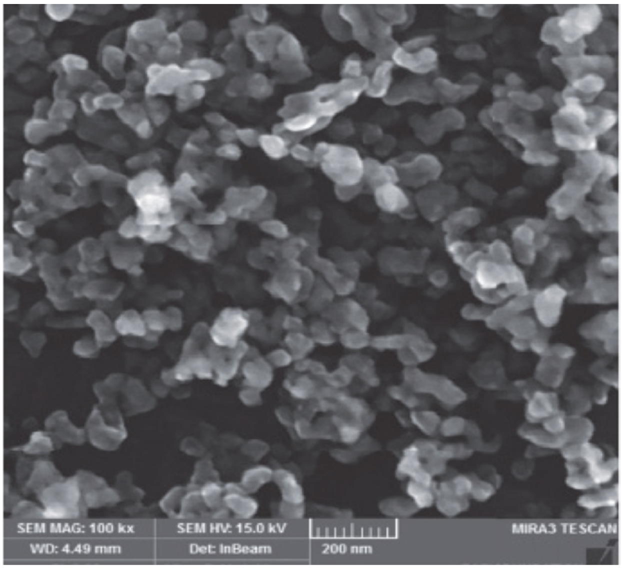

Figure 4. Field emission scanning electron microscopy (FESEM) micrograph of Fe_3O_4@$PyHBr_3$ MNP.

lower than that of pure Fe_3O_4-MNP (74 emu g^{-1}) (not shown here). The decrease in the measured saturation magnetization was due to the presence of organics around Fe_3O_4.

The thermal stability of the Fe_3O_4 MNPs and Fe_3O_4@ $PyHBr_3$ MNPs was also investigated. Comparison of the respective thermograms showed that no significant weight loss was observed for the Fe_3O_4 thermogram (Figure 5, black thermogram). On the other hand, the thermograms of Fe_3O_4@$PyHBr_3$ showed three weight loss steps of about 15 % in the range of 200–600 °C, which could be attributed to the evaporation of residues trapped in the samples and the removal of the organic content.

The oxidation of alcohol is one of the most important reactions in the synthesis of organic compounds.[30–38] Some of these reactions occur under difficult conditions, such as high temperatures, the use of unfavorable solvents, and the use of toxic oxidizing agents, including transition metal compounds that produce harmful byproducts. Usually, compounds such as chromic acid, di-

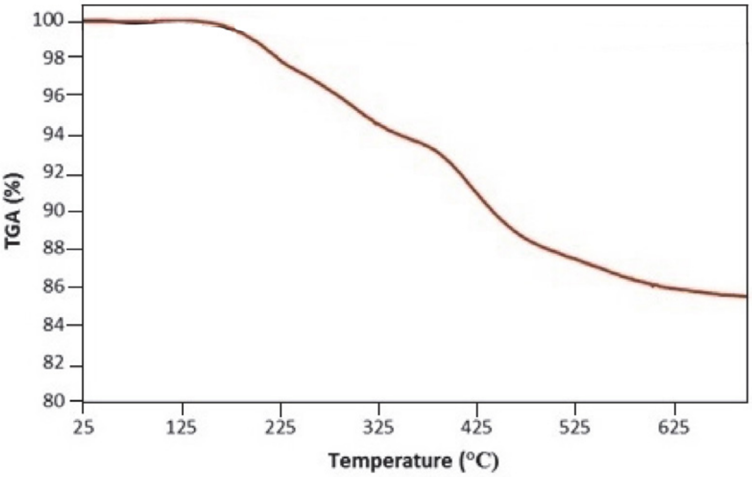

Figure 5. Thermograms of pure Fe_3O_4 MNPs (black) and Fe_3O_4 @ $PyHBr_3$ MNPs (red).

chromate/H^+, PCC, PDC are used to oxidize alcohols.[34] Due to the limitations of existing methods, efforts are being made to perform environmentally friendly reactions. The goal of these efforts is to catalytically oxidize alcohols using low-cost green oxidants such as air, oxygen, and hydrogen peroxide, and using heterogeneous (solid) catalysts and harmless and environmentally friendly solvents. Hydrogen peroxide (H_2O_2) is an attractive oxidant for liquid-phase reactions.[34–38] This water-soluble oxidant is safe, inexpensive, and has a high oxygen content that does not require a buffer. In addition, it is considered a green and environmentally friendly oxidant because it releases water as a byproduct. After the synthesis of pyridinium hydrotribromide on Fe_3O_4 MNP, we investigated the effectiveness of Fe_3O_4@PyHBr$_3$ MNP as a catalyst in the oxidation of benzyl alcohols with 30% hydrogen peroxide. To optimize the reaction conditions, the oxidation of 4-bromobenzyl alcohol with different amounts of 30% hydrogen peroxide, different amounts of Fe_3O_4@PyHBr$_3$ catalyst and different reaction temperatures were investigated (Scheme 2).

To determine the optimum amount of hydrogen peroxide, the reaction of 4-bromobenzyl alcohol (1 mmol) in various molar ratios of H_2O_2 to alcohol was studied in the presence of 0.020 g catalyst at 50 °C in H_2O (1 mL) (Table 1, entries 1–4). According to the results, it was found that the reaction had a higher conversion (60 %) and a shorter time (60 minutes) when 4 mmol of H_2O_2 was used, but this time additional amounts of catalyst were used to increase the conversion (Table 1, entries 5–6 and 9). The results show that increasing the amount of catalyst leads to an increase in conversion. The effects of reaction temperature were also studied (Table 1, entries 6–8). At 25 °C and 70 °C, the conversions were 65 % and 90 %, respectively.

The reaction was also carried out with Fe_3O_4 (0.23 g), and it was found that the reaction time was longer than that of the Fe_3O_4@PyHBr$_3$ catalyst (Table 1, entry 11). When the reaction was carried out without catalyst, the desired product was produced after 4 hours with a very low conversion (Table 1, entry 12).

According to the results in Table 1, the optimum conditions for this reaction are 4 mmol 30% hydrogen peroxide as oxidant, 0.070 g (9.1 mol%) Fe_3O_4@PyHBr$_3$ as catalyst at 50 °C (Table 1, entry 6). Under these optimum conditions, 4-bromobenzaldehyde was obtained in 20 min with an excellent conversion rate of 100 %. The reaction of benzyl alcohol and other benzyl alcohols with electron donor and electron acceptor substituents was carried out under these optimum conditions, and the results are shown in Table 2. Benzyl alcohols with electron donor group (Table 2, entries 2, 6, 7, 9) were oxidized in shorter time than alcohols with strong electron acceptor group (Table 2, entries 8, 10, 11). The secondary benzyl alcohols (entries 13 and 14) were also oxidized to the corresponding ketones. The study showed that the oxidation time of the non-benzyl alcohol 2-phenyl-1-propanol was longer than that of the benzyl alcohols (Table 2, entry 12). Moreover, no additional oxidation to the carboxylic acid was observed for the primary alcohols, which is one reason for the mildness and selectivity of the present method.

After the reaction was completed, the catalyst was separated with a magnet. To evaluate the performance of Fe_3O_4@PyHBr$_3$ catalyst after recovery, the catalyst used in each reaction was separated with a magnet and reused in the next reaction after rinsing with CH_2Cl_2 (3 × 5 ml). The catalyst recovery results for the oxidation of 4-bromobenzyl alcohol showed that the catalyst could be used for up to 5 cycles without significantly reducing the reaction yield (Table 3).

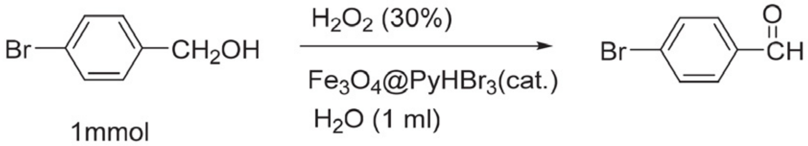

Scheme 2. Oxidation of 4-bromobenzyl alcohol by hydrogen peroxide in the presence of Fe_3O_4@ PyHBr$_3$.

Table1. Optimization of **the** oxidation of 4-bromobenzyl alcohol by 30% H_2O_2.[a]

Entry	H_2O_2/alcohol Molar ratio	Catalyst (g)	T (°C)	Reaction time (min)	Conversion (%)
1	1	0.02	50	120	30
2	2	0.02	50	120	45
3	3	0.02	50	90	50
4	4	0.02	50	60	60
5	4	0.04	50	45	80
6	4	0.07	50	20	100
7	4	0.07	25	60	65
8	4	0.07	70	20	90
9	4	0.08	50	18	100
10	3	0.07	50	40	80
11	4	0.23[b]	50	40	96
12	4	–	50	240	5

[a] The reaction was performed using 4-bromobenzyl alcohol (1 mmol) in H_2O (1 mL). [b] Fe_3O_4 MNP were used as a catalyst.

Table 2. Fe_3O_4@ $PyHBr_3$ MNP catalyze the oxidation of alcohols to carbonyl compounds.[a]

Entry	Substrate	Product	Reaction Time (min.)	yield[b] (%)
1	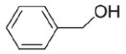	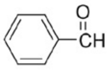	20	88
2	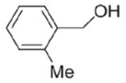	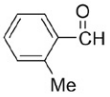	10	95
3	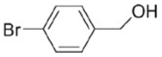	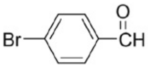	20	95
4	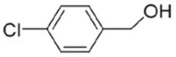	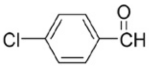	30	93
5	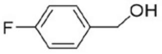	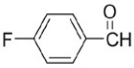	35	90
6	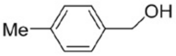	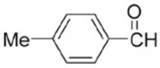	25	98
7	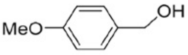	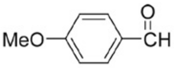	15	90
8	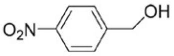	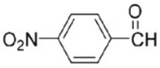	75	85
9	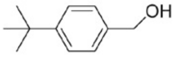	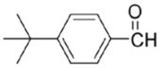	18	86
10	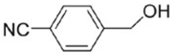	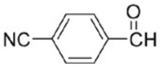	60	97
11	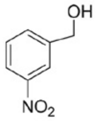	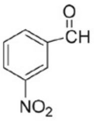	60	88
12	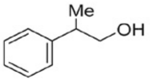	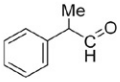	80	91
13	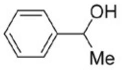	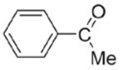	35	94
14	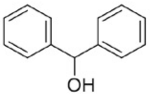	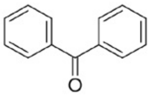	10	95

[a] Reaction conditions: substrate (1 mmol), Fe_3O_4@ $PyHBr_3$ MNP (0.07 g, 9.1 molar%), aqueous hydrogen peroxide (4 mmol, 30%), H_2O (1 mL), at 50 °C. [b] Isolated yields.

Table 3. Recyclability of Fe_3O_4@$PyHBr_3$ catalyst.

Run	1	2	3	4	5
Yield (%)	95	90	88	85	80
Time (min)	20	20	20	20	20

The efficiency of this catalyst can also be illustrated by comparing the results obtained in this study for the oxidation of benzyl alcohol with those published in the literature. For this purpose, several recent methods are given in Table 4 along with the temperature, reaction time, and yield.

Table 4. Comparison of the present method with other methods reported for the oxidation of benzyl alcohol.

Reagents	**Reaction time (min)**	**Temperature (°C)**	**Yield%**
PVP-Br_3	70	r.t.	94[17]
Silica-supported *DABCO-Br_3	60	80	95[24]
H_2O_2 (1.1 eq), $\{[K.18\text{-Crown-}6]Br_3\}_n$	30	80	81[36]
H_2O_2 (3 eq), **DBDMH (0/5 eq)	120	60	85[37]
H_2O_2 (1.3eq), $MgFe_2O_4$ MNPs	55	60	88[38]
H_2O_2, $K_8[BW_{11}O_{39}H]_{13}H_2O$	360	90	98[34]
H_2O_2,VHPW/MCM-41/NH_2	480	80	97[35]
H_2O_2, Fe_3O_4@PyHBr_3	20	50	88[this work]

*DABCO =1,4-diazabicyclo[2.2.2]octane **DBDMH= 1,3-Dibromo-5,5-dimethylhydatoin

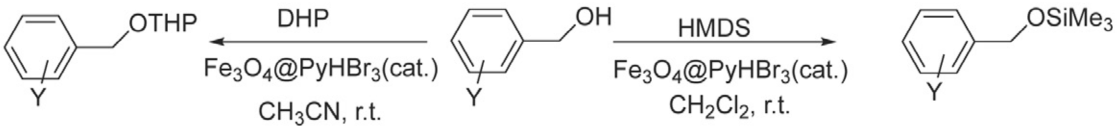

Scheme 3. Trimethylsilylation and tetrahydropyranylation of benzyl alcohols in the presence of Fe_3O_4@PyHBr_3

Trimethylsilylation and tetrahydropyranylation of benzyl alcohols were studied in the presence of Fe_3O_4@PyHBr_3 (Scheme 3). According to the optimum conditions obtained for 4-bromobenzyl alcohol, trimethylsilylation of various alcohols was carried out with Fe_3O_4@PyHBr_3 (0.07 g, 9.1 mol%), HMDS (0.7 mmol) in CH_2Cl_2 (5 mL) at room temperature (Scheme 3, Table 5). Tetrahydropyranylation of alcohols was also carried out with Fe_3O_4@PyHBr_3 (0.07 g, 9.1 mol%), DHP (1.5 mmol) in CH_3CN (5 mL) at room temperature (Scheme 3, Table 5).

These results show that for all types of benzyl alcohols with electron donor and electron acceptor substituents, the corresponding trimethylsilyl ethers were obtained in short time and in excellent yield. The reaction times are shorter for benzyl alcohols with electron donor substituents than for benzyl alcohols with strong electron acceptor substituents.

These results showed that the corresponding tetrahydropyranyl ethers were obtained in high yields for primary benzyl alcohols with electron acceptor or electron donor substitutions. However, the reaction times were shorter for benzyl alcohols with electron donor substitutions.

4. Conclusions

In summary, the magnetic Fe_3O_4@PyHBr_3 nanocatalyst was prepared and characterized by FTIR, CHN, TGA, XRD, FE-SEM and VSM analyzes. The efficiency of this magnetic nanocatalyst in the oxidation reaction of alcohols to aldehydes and ketones was investigated. The results showed that Fe_3O_4@PyHBr_3 was very effective as a catalyst in the oxidation of alcohols using H_2O_2 as a green oxidant. This method has some advantages, such as very mild reaction conditions, easy separation and reusability of the catalyst, very short reaction times, high yields, and the use of H_2O as a green solvent. No additional oxidation to the carboxylic acid was observed for the primary alcohols, which is one reason for the mildness and selectivity of the present method. The use of this magnetic catalyst in the reactions of trimethylsilylation and tetrahydropyranylation of alcohols was also studied, and it was found to have many advantages, such as easy separation of the catalyst, good yields, and mild reaction conditions.

Acknowledgment

The authors gratefully acknowledge financial support for this work from Damghan University.

5. References

1. B. Han, Z. Zheng, D. Zheng, L. Zhang, P. Cui, J. Shi, C. Li, *Synth. Commun.* **2019**, *49*, 2512–2520. **DOI:**10.1080/00397911.2019.1631348
2. S. Gao, T. K. Bethel, T. Kakeshpour, G. E. Hubbell, J. E. Jackson, J. J. Tepe, *J. Org. Chem.* **2018**, *83*, 9250–9255. **DOI:**10.1021/acs.joc.8b01251
3. R. R. Dey, B. Paul, S. S. Dhar, *Synth. Commun.* **2015**, *45*, 714–726. **DOI:**10.1080/00397911.2014.979509
4. D. Bliman, M. Pettersson, M. Bood, M. Grøtli, *Tetrahedron Lett.* **2014**, *55*, 2929–2931. **DOI:**10.1016/j.tetlet.2014.03.084
5. M. Simurdiak, O. Olukoga, K. Hedberg, *J. Chem. Edu.* **2016**, *93*, 322–325. **DOI:**10.1021/acs.jchemed.5b00283

Table 5. $Fe_3O_4@PyHBr_3$ MNP-catalyzed trimethylsilylation and tetrahydropyranylation of alcohols.

Entry	Substrate	Trimethylsilylation[a] Time (min)	Trimethylsilylation[a] Yield[c] (%)	Tetrahydropyranylation[b] Time (min)	Tetrahydropyranylation[b] Yield[c] (%)
1	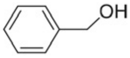	10	92	120	86
2	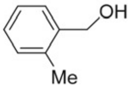	12	85	150	80
3	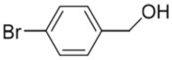	10	95	120	96
4	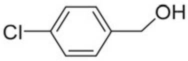	20	88	180	94
5	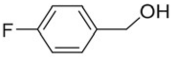	25	96	200	87
6	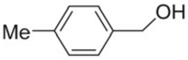	10	94	120	92
7	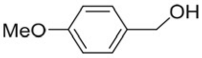	8	96	90	98
8	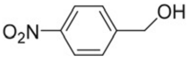	45	80	245	80
9	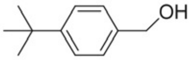	10	88	100	95
10	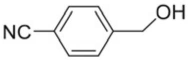	30	80	175	90
11	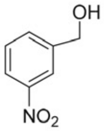	35	86	210	75
12	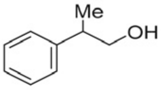	20	80	240	70
13	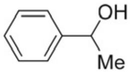	50	82	240	70
14	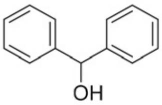	30	89	150	85

[a] Reaction conditions: substrate (1 mmol), Fe_3O_4@ $PyHBr_3$ (0.07 g, 9.1 molar%), HMDS (0.7 mmol), CH_2Cl_2 (5 mL), at room temperature. [b] Reaction conditions: substrate (1 mmol), Fe_3O_4@ $PyHBr_3$ (0.07 g, 9.1 molar%), DHP (1.5 mmol), CH_3CN (5 mL), at room temperature. [c] Isolated yield.

6. S.-H. Yang, *Synlett* **2009**, *8*, 1351–1352. **DOI:**10.1055/s-0029-1216645
7. M. Dey, S. S. Dhar, M. Kalita, *Synth. Commun.* **2013**, *43*, 1734–1742. **DOI:**10.1080/00397911.2012.666694
8. J. K. Joseph, S. L. Jain, B. Sain, *Catal. Commun.* **2007,** *8*, 83–87. **DOI:**10.1016/j.catcom.2006.05.035
9. P. Gogoi, S. Hazarika, P. Barrman, *RSC Adv.*, **2015,** *5*, 38044–38047. **DOI:**10.1039/C5RA04573H

10. M. Dey, R. R. Dey, S. S. Dhar, *Chem. Lett.* **2014**, *43*, 631–633. **DOI:**10.1246/cl.131192
11. M. Dey, S. S. Dhar, *Green Chem. Lett. Rev.* **2012**, *5*, 639–642. DOI: **DOI:**10.1080/17518253.2012.692820
12. R. R. Dey, B. Paul, S. S. Dhar, S. Bhattacharjee, *Chem. Lett.* **2014**, *43*, 1545–1547. **DOI:**10.1246/cl.140564
13. A. R. Hajipour, S. A. Pourmousavi, A. E. Ruoho, *Synth. Commun.* **2005**, *35*, 2889–2894. **DOI:**10.1080/00397910500297297
14. L. Wu, X. Yang, *Phosphorus, Sulfur Silicon Relat. Elem.* **2012**, *187*, 748–753. **DOI:**10.1080/10426507.2011.616561
15. A. R. Hajipour, S. A. Pourmousavi, A. E. Ruoho, *Phosphorus, Sulfur Silicon Relat. Elem.* **2007**, *182*, 921–937. **DOI:**10.1080/10426500601088739
16. A. Kharazmi, R. Ghorbani-Vaghei, S. Alavinia, *ChemistrySelect* **2020**, *5*, 1424–1430. **DOI:**10.1002/slct.201904697
17. A. Ghorbani-Choghamarani, M. Nikoorazm, B. Tahmasbi, M. Norouzi, *J. Saudi Chem. Soc.* **2017**, *21*, 408–414. **DOI:**10.1016/j.jscs.2015.08.002
18. N. E. Sodan, A. Hol, O. Caylak, L. Elci, *Acta Chim. Slov.* 2020, 67, 375–385. **DOI:**10.17344/acsi.2018.4636
19. O. Arjmand, M. Ardjmand, A. M. Amani, M. H. Eikani, *Acta. Chim. Slov.* 2020, 67, 496–506. **DOI:**10.17344/acsi.2019.5513
20. K. Vasic, Z. Knez, S. Kumar, J. K. Pandey, M. Leitgeb, *Acta Chim. Slov.* 2020, 67, 1172–1179. **DOI:**10.17344/acsi.2020.6065
21. M. Ghobadi, P. Pourmoghaddam Qhazvini, M. Eslami, M. Kazemi, *Synth. Commun.* **2021**, *51*, 325–350. **DOI:**10.1080/00397911.2020.1829646
22. L. Shiri, M. Kazemi, *Phosphorus, Sulfur Silicon Relat. Elem.,* **2017**, *192*, 1171–1176. **DOI:**10.1080/10426507.2017.1347654
23. A. Rostami, Y. Navasi, D. Moradi, A. Ghorbani-Choghamarani, *Catal. Commun.* **2014**, *43*, 16–20. **DOI:**10.1016/j.catcom.2013.08.025
24. F. Matloubi Moghaddam, N. Masoud, B. Koushki Foroushani, S. Saryazdi, N. Ghonouei, E. Daemi, *Sci. Iran., Trans. C: Chem.Chem. Eng.* **2013**, *20*, 598–602. **DOI:**10.1016/j.scient.2013.02.015
25. M. Ghobadi, M. Kargar Razi, R. Javahershenas, M. Kazemi, *Synth. Commun.* **2021,** *51*, 647–669. **DOI:**10.1080/00397911.2020.1819328
26. J. Govan, Y. K. Gun'ko, *Nanomaterials,* **2014**, *4*, 222–241. **DOI:**10.3390/nano4020222
27. U. Bora, M. K. Chaudhuri, D. Dey, S. S. Dhar, *Pure Appl. Chem.* **2001**, *73*, 93–102. **DOI:**10.1351/pac200173010093
28. R. Borah, A. J. Thakur, *Synth. Commun.* **2007**, *37*, 933–939. **DOI:**10.1080/00397910601163794
29. Z. Zarnegar, J. Safari, *J. Mol. Struc.*, **2014**, *1072*, 53–60. **DOI:**10.1016/j.molstruc.2014.04.023
30. Q. L. Luo, W. H. Nan, Y. Li, X. Chen, *ARKIVOC* **2014**, (*iv*), 350–361. **DOI:**10.3998/ark.5550190.p008.707
31. A. R. Pourali, M. Tabaean, S. M. R. Nazifi, *Chin. Chem. Lett.* **2012**, *23*, 21–24. **DOI:**10.1016/j.cclet.2011.07.022
32. S. Bahrami-Nasab, A. Pourali, *Curr. Chem. Lett.* **2014**, *3*, 43–48. **DOI:**10.5267/j.ccl.2013.10.004
33. M. A. Zolfigol, A. R. Pourali, S. Sajjadifar, S. Farahmand, *Curr. Catal.* **2013**, *8*, 151–158. **DOI:**10.2174/2211544711302020009
34. X. Dong, D. Wang, K. Li, Y. Zhen, H. Hu, G. Xue, *Mater. Res. Bull.* **2014**, *57*, 210–220. **DOI:**10.1016/j.materresbull.2014.05.041
35. W. Zhao, Y. Zhang, B. Ma, Y. Yong Ding, W. Qiu, *Catal. Commun.* **2010**, *11*, 527–531. **DOI:**10.1016/j.catcom.2009.12.010
36. M. Rasouli, M. A. Zolfigol, M. H. Moslemin, G. Chehardoli, *Green Chem. Lett. Rev.* **2017**, *10*, 117–120. **DOI:**10.1080/17518253.2017.1306614
37. J. Lee, J. C. Lee, *Lett. Org. Chem.* **2018**, *15*, 895–898. **DOI:**10.2174/1570178615666180613080548
38. F. Sadri, A. Ramazani, H. Ahankar, S. Taghavi Fardood, P. Azimzadeh Asiabi, M. Khoobi, S. Woo Joo, N. Dayyani, *J. Nanostruct.* **2016**, *6*, 264–272. **DOI:** 10.22052/JNS.2016.41621

Povzetek

V raziskavi je bil v treh korakih sintetiziran nov magnetni nanokatalizator na osnovi nanodelcev železovega oksida, povezanih s piridinijevim hidrotribromidom (Fe_3O_4@PyHBr$_3$). V prvi stopnji so 3-(aminopropil)trietoksisilan (APTES) reagirali s 4-(bromometil)piridin hidrobromidom. V drugem koraku pa so produkt prve stopje reagirali z nanodelci železovega oksida. V zadnjem koraku so izvedli reakcijo s pomočjo mletja s KBr in HIO_4 v mlinu, in nanokatalizator Fe_3O_4@PyHBr$_3$ okarakterizirali s FT-IR, CHN, XRD, SEM, TGA in VSM analizo. Magnetni nanokatalizator je bil uporabljen kot katalizator za selektivno oksidacijo alkoholov v aldehide in ketone z uporabo 30 % H_2O_2 kot oksidanta. Reakcija je potekla v kratkem času in z visokimi izkoristki, poleg tega pa niso opazili nadaljnje oksidacije alkoholov. Magnetni nanokatalizator so učinkovito reciklirali v petih zaporednih ciklih brez pomembnejše izgube katalitične aktivnosti. Prav tako so z njim uspešno izvedli trimetilsililiranje in tetrahidropiranilizacijo alkoholov.